Green Chemistry

PAPER

View Article Online
View Journal | View Issue

Cite this: *Green Chem.*, 2026, **28**, 1960

Lifecycle cost, environmental, and machine-learning value assessment for synthetic spider silk production from *E. coli*

Melika Tajipour,[a] Bojing Jiang,[b] Leo Penny,[b] Pallavi Dubey,[a] Hayley Wabiszewski,[c] Fuzhong Zhang,[b] Marcus Foston[b] and Mark Mba Wright[*a]

Synthetic spider silk biomaterials with exceptional strength and thermal resistance have attracted growing interest for various applications, including the textile and medical industries. Natural spider silk production relies on farming spiders, which poses technical, economic, environmental, and ethical challenges. Synthetic spider silk offers an alternative path to high-quality silk materials. However, there is limited information on the costs and environmental benefits of synthetic spider silk. This study employs techno-economic analysis (TEA) and life cycle assessment (LCA) to evaluate the economic feasibility and environmental impact of large-scale synthetic spider silk manufacturing. Experimental data are based on *Escherichia coli* (*E. coli*) to produce recombinant spider silk proteins. A commercial-scale fiber production facility was simulated in BioSTEAM. Environmental impacts were assessed using OpenLCA. Our findings reveal that the production of synthetic spider silk can achieve a minimum sale price of 14.96 USD to 87.8 USD per kilogram, with associated greenhouse gas emissions (GHG) of 17.39 to 104.11 kg CO_2e per kilogram. The machine learning analysis indicates that synthetic fiber market values could range between 5 and 25 USD per kilogram. Sensitivity analysis indicates that fiber yield, glycerol, and urea are the most important economic and environmental factors. Synthetic spider silk could become a competitive and environmentally friendly material for various industries by optimizing production processes for greater fiber yield and identifying novel raw materials.

Received 25th September 2025,
Accepted 15th December 2025

DOI: 10.1039/d5gc05082k

rsc.li/greenchem

Green foundation

1. We provide the first integrated techno-economic, life cycle, and machine-learning assessment of synthetic spider silk, demonstrating its potential as a low-carbon alternative to animal-derived and petroleum-based fibers.
2. Our study shows that synthetic silk can be produced with GHG emissions as low as 18 kg CO_2e per kg fiber, a 70% reduction compared to natural silk (≈58 kg CO_2e per kg), while achieving minimum selling prices of ~$15 per kg in optimized yields.
3. Future research should focus on increasing the fiber yield, reducing reliance on high-impact inputs like glycerol and urea, and integrating renewable or waste-derived feedstocks, as well as recovery/reuse of solvents and buffers.

1. Introduction

Spider silk, renowned for its exceptional strength and biocompatibility, presents a compelling alternative because its mechanical properties surpass those of silkworm silk and other fiber materials, making it a prime candidate for biomaterial applications.[1–3] Global silk production from 2011 to 2022 ranged between 86 000 and 200 000 metric tons per year.[4] However, the challenges associated with scalable production and harvesting of natural spider silk have led researchers to focus on producing recombinant spider silk proteins using transgenic organisms.[5–7]

Many challenges limited the cost-effective production of recombinant spider silk, including genetic instability of highly repetitive gene sequences, low protein yield due to the ultra-high molecular weight of silk proteins, scalable protein purification and fiber spinning processes, *etc.*[8–10] Although a wide range of transgenic organisms have been explored,[11] heterologous production of recombinant or synthetic silk fibers with mechanical properties on par with natural spider silk

[a]*Department of Mechanical Engineering, Iowa State University, Ames, IA 50011, USA. E-mail: markmw@iastate.edu*
[b]*Department of Energy, Environmental & Chemical Engineering, Washington University in St Louis, St Louis, MO 63130, USA*
[c]*School of Business, The University of Utah, Salt Lake City, UT 84112, USA*

fiber was only recently demonstrated using engineered *Escherichia coli.*[12,13,14] *Escherichia coli*, a widely used microbial host for industrial recombinant protein production, offers several advantages for producing synthetic spider silk. These include its rapid growth rate, the ability to use cheap and renewable feedstock, readily available genetic tools, and extensive knowledge on its systems biology related to recombinant protein production. These attributes contribute to economic viability by enabling high cell densities and economically viable growth on inexpensive media such as glucose, which can reduce production costs significantly in scaled-up processes, with optimized scenarios achieving minimum selling prices as low as $23 per kg.[10,15] Environmentally, *E. coli*-based production supports sustainability by yielding lower greenhouse gas emissions (55 kg CO_2-eq. per kg in optimized cases) compared to natural silk harvesting and facilitates the use of non-harmful solvents and renewable resources, making it a more balanced alternative to animal-derived silk.[10,15]

Moreover, *E. coli* supports large-scale production, addressing the challenge of producing sufficient quantities of spider silk for commercial use. The efficient expression systems in *E. coli* enhance the yield and quality of the recombinant silk proteins, while its relatively straightforward purification processes ensure high-quality silk suitable for various applications. These properties make *E. coli* an ideal organism for overcoming the production challenges associated with natural spider silk, enabling the creation of synthetic spider silk with desirable mechanical properties.[16–21,44] In synthetic spider silk production, researchers mimic the spinning process using methods like wet spinning, where recombinant silk proteins are extruded through a spinneret into a coagulation bath, often containing methanol or isopropanol, to form fibers.[22,23] Wet spinning is cost-effective due to efficient production from low-protein-concentration dopes, minimizing material use and enabling high yields of fibers with excellent mechanical properties. This method is environmentally beneficial as it avoids toxic solvents, relying on water-based systems that reduce pollution and support biodegradability, positioning it as a greener alternative to traditional synthetics.[24]

Synthetic methods can produce fibers with properties comparable to natural silk, but achieving the same mechanical qualities remains challenging, requiring post-spinning processes such as additional drawing steps to enhance fiber strength and toughness.[25] Current laboratory methods for fabricating silk and its derivatives are both labor-intensive and costly, making them impractical for commercial production.[26] Despite efforts by several companies to scale up spider silk production through fermentation, their achievements are limited to prototype garments and small product runs like ties, indicating that substantial industrial-scale production has not yet been realized.[27] To ensure the feasibility of producing spider silk in large quantities, it is essential to transition from laboratory to industrial-scale production. This transition must be evaluated for its commercial viability and sustainability through comprehensive techno-economic analysis (TEA) and life cycle assessment (LCA), given the high costs associated with the materials and production processes.[10,15]

Knowledge on the cost of synthetic silk fibers and their environmental benefits remains limited. Edlund *et al.* investigated the economic feasibility and environmental impact of silk fibers from *E. coli.*[10] Their study determined that fiber production costs ranged from $23 to $761 per kg, depending on the manufacturing scale and process optimization. Their LCA focused on greenhouse gases (GHG) and estimated GHG emissions to range between 55 and 572 kg CO_2e per kg of fiber. To our knowledge, this is the only study focused on synthetic silk fibers. Khan and Dandautiya *et al.* published a review in 2023 on silk production LCA studies.[28] They identified two studies showing that conventional silk fiber estimates ranged from 80.9 to 25 425 kg CO_2e per kg.[29,30] The synthetic silk scientific literature would benefit from additional LCAs.

The aim of this study is to evaluate the commercial feasibility and environmental impact of large-scale synthetic spider silk production. To set up a TEA model that can best capture the current synthetic silk fiber production process, we performed fed-batch fermentation and protein purification to obtain titers and yield of purified proteins from the fermentation process. These experimental data were then used to simulate large-scale silk fiber manufacturing. This model was constructed to enable a comprehensive assessment of the production process, focusing on both economic viability and environmental sustainability. Our analysis is based on *E. coli* fermentation and evaluates costs and GHG emissions, similar to Edlund *et al.*[10] We expand on the previous work by investigating new experimental results, innovations in post-fermentation processing, and machine-learning based predictions of fiber values. The scientific contributions of this study include the detailed process design and commercial feasibility evaluation of synthetic silk fiber production, lifecycle assessment of synthetic fibers, and machine learning predictions of synthetic fiber market prices. The study includes scenario and sensitivity analysis to identify key parameters and opportunities for future development.

2. Methodology

2.1. Synthetic silk fiber biorefinery design

This study evaluates the economic and environmental performance of a commercial-scale synthetic silk fiber biorefinery. The study employs an N^{th} plant design basis.[31] This basis assumes that the scientific and technological breakthroughs required for commercialization have been addressed, and the facility operates as reliably as a mature biorefinery. Potential scale-up challenges are discussed in relevant sections below. The biorefinery produces between 1200 and 9000 metric tons per year of silk fiber, depending on the fiber yield. These capacities are comparable to those reported in previous studies,[10] and they are similar to specialty fiber plant capacities.[32,33] The biorefinery consists of three main sections: cell culture, protein recovery, and fiber processing. Cell culture

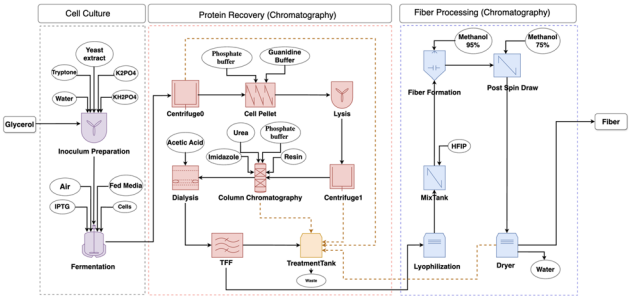

Fig. 1 Simplified process flow diagram for synthetic spider silk production from *E. coli*. Colors indicate the process section (purple: cell culture; red: protein recovery; blue: fiber processing). Waste streams shown as dashed lines.

includes inoculum preparation and fermentation using glycerol, fed and batch media, and various specialty chemicals. Protein recovery employs various mechanical and chemical formation, separation, and recovery steps. Fiber processing takes raw, wet fiber proteins and uses alcohols and thermomechanical steps to yield a bulk market quality fiber product. The overall diagram is illustrated in Fig. 1.

2.2. Synthetic silk protein production

To obtain the titer, yield, and rate of synthetic silk protein production for TEA analysis, we performed fed batch fermentation using a previously engineered synthetic silk protein ^{N}M-16xFGA-^{C}M (RSSP) and *E. coli* BL21(DE3) cell as the production host.[14,34] Seed culture was cultivated in Terrific Broth (TB) containing 50 μg mL^{-1} kanamycin following previous protocols.[35–37] Specifically, 500 mL of seed culture grew at 37 °C with shaking until its optical density (OD600) reached approximately 5. Cells were then centrifuged and resuspended in 1 L of batch media containing 10 g L^{-1} glucose, 60 g L^{-1} glycerol, 20 g L^{-1} tryptone, 24 g L^{-1} yeast extract, and minerals, such as potassium and sodium phosphates, which stabilized the pH during high metabolic activity. Trace minerals, including ferric citrate, cobalt chloride, and manganese chloride, were added to promote cellular enzymatic function.

The cell suspension was then transferred to a 2 L Bioflo120 fed-batch bioreactor for fermentation. The system maintained a constant temperature of 29 °C and pH of 7.1, adjusted with either 3 M phosphoric acid or 25% ammonia. Aeration was optimized with a dissolved oxygen (DO) level initially set to 70% and maintained above 30% by adjusting stirring speeds from 200 to 1200 rpm and regulating the airflow. At an OD600 of approximately 68, induction was triggered by adding IPTG to a final concentration of 0.25 mM. A nutrient-rich feed solution (400 g L^{-1} glycerol, 20 g L^{-1} tryptone, 24 g L^{-1} yeast extract, and mineral salts consisting of 13.3 g L^{-1} KH_2PO_4, 4.0 g L^{-1} K_2HPO_4, 1.7 g L^{-1} NaCl, 1.0 g L^{-1} $(NH_4)_2SO_4$, and 0.5 g L^{-1} $MgSO_4{\cdot}7H_2O$, together with trace minerals including 0.016 g L^{-1} ferric citrate, 0.0024 g L^{-1} $CoCl_2{\cdot}6H_2O$, and 0.0015 g L^{-1} $MnCl_2{\cdot}4H_2O$) was continuously supplied at 0.2 mL min^{-1} to sustain cell growth and protein expression. The feed rate was controlled to balance the metabolic load and avoid substrate inhibition. Cell pellets were harvested 20 hours post-induction to maximize the recombinant protein yield.

2.3. Protein extraction and purification

Protein was purified using affinity chromatography following previous methods with slight modifications. Specifically,[8,38] cell pellets were lysed in buffer A (6 M guanidine hydrochloride, 50 mM K_2HPO_4, and 300 mM NaCl, pH 7.0) at a ratio of 1500 mL per liter of cell culture. The cell lysate was then centrifuged to separate the cell debris, and the supernatant containing target proteins was subjected to affinity purification using Ni-NTA resin. After loading, the column was washed with buffer B (8 M urea, 50 mM K_2HPO_4, and 300 mM NaCl, pH 7.0) containing increasing imidazole concentrations (0 mM, 20 mM, and 50 mM) followed by protein elution using buffer C (8 M urea, 50 mM K_2HPO_4, and 300 mM NaCl, 300 mM imidazole, pH 7.0). The eluate protein was dialyzed against 1% acetic acid and subsequently lyophilized. The purified material was stored at −80 °C until further processing.

2.4. Fiber formation process

For fiber formation, the lyophilized protein powder was dissolved in hexafluoro isopropanol (HFIP) to create a 15 wt% solution. The protein dope was loaded into a syringe fitted with a 23G needle and extruded into a 95% v/v methanol bath at a controlled rate of 10 μL min^{-1} using a syringe pump. Methanol induced rapid solidification, forming a stable fiber protein.

This study employs laboratory data to determine equipment configurations, select operating conditions, and define operating performance parameters. To our knowledge, there are no commercial synthetic silk fiber facilities using the approach described in this study. Commercial-scale operation could involve several tradeoffs: (1) a commercial facility may seek lower cost chemical alternatives that may decrease fiber yields; (2) large-scale equipment may pose mass and heat transfer limitations; (3) impurities and the inherent variability of the biological process could result in lower yields; (4) material and heat recovery may be required to reduce costs; (5) wastewater treatment may be required to handle specialty chemicals. These challenges are common to many fermentation processes, and they have been addressed in similar applications.[33] To our knowledge, no major barriers have been identified that would limit the technical feasibility of the process. However, costs and environmental performance of a first-of-a-kind facility may differ from those estimated in this study.[39]

2.5. Techno-economic analysis

The extruded fibers underwent mechanical drawing, extending to seven times their original length in an 80% methanol bath to enhance tensile properties. Once stretched, fibers were air-dried under controlled humidity and temperature conditions.

The TEA feasibility of the commercial-scale synthetic silk fiber production facility was assessed using a standard set of financial assumptions. These assumptions, applied in con-

Table 1 Financial assumptions for a synthetic silk fiber biorefinery (adapted from ref. 31 and 40)

Parameter	Value
Internal rate of return	10%
Project lifetime	20 years
Income tax	21%
Operating days	330 days per year
Lang factor	4.5
Finance fraction	40%
Finance duration	10 years
Depreciation schedule	MACRS 7-year

junction with the process model, facilitate a comprehensive understanding of the economic viability of industrial-scale synthetic spider silk production, as shown in Table 1. Key economic parameters include an internal rate of return (IRR) of 10%, a project duration spanning from 2018 to 2038, and equipment depreciation following the Modified Accelerated Cost Recovery System (MACRS) 7-year schedule. An income tax rate of 21% was applied in this study, with operations assumed to run for 330 days annually. The working capital was set at 5% of the fixed capital investment (FCI), while labor costs include a 40% charge to account for fringe benefits. Other financial assumptions included property tax at 0.1%, property insurance at 0.5%, and maintenance costs at 0.3% of the total investment.

Operating costs are based on various assumptions for material, utility prices, labor rates, and miscellaneous costs. Table 2 shows material and chemical price assumptions. Material prices were gathered from online sources and represent averages of industrial-grade prices from January to May 2025. Vendor prices are subject to change over time. The electricity price is 7.82 cents per kWh which is comparable to U.S. industrial power prices. The steam price is 1.3 cents per kg of steam. Labor rates are scaled linearly based on the study by the National Renewable Energy Laboratory (NREL).[41]

Table 2 also provides the GHG impact factor associated with various chemicals used in the synthetic spider silk production process. Glycerol stands out as the most significant contributor with an emission factor of 12 kg CO_2 per kg, highlighting its substantial environmental impact. HFIP follows with a notable impact of 10 kg CO_2 per kg. Other materials such as isopropanol and glucose also contribute significantly, with impact factors of 3.21 and 1.3 kg CO_2 per kg, respectively. Essential nutrients and compounds like urea, IPTG, PBS, and Na_2SO_4 show moderate impact factors ranging from 0.5 to 1.87 kg CO_2 per kg. Conversely, chemicals like yeast, NaClO, and NH_4Cl exhibit minimal impact, reflecting their relatively lower contributions to the overall GHG emissions. A complete lifecycle inventory table is available in the SI (Table S1).

2.6. Life cycle assessment

Life Cycle Assessment (LCA) is a widely recognized and practical approach used to evaluate the health and environmental impacts of a product system, starting from raw material extraction, continuing through production and consumption, and ending with the disposal or recycling of the final product. The Cradle-to-Gate approach was chosen for this study to focus specifically on the impacts occurring within the production phase of the system. Global Warming Potential (GWP) has been considered as the impact factor and using carbon dioxide equivalent (CO_2-eq) as a metric.[29] This metric allows for the aggregation of different GHGs into a single value, simplifying the assessment and comparison of their impact on global warming. This approach matches the LCA by Edlund *et al.*[10] In this study, the EcoInvent 3.7.1 database was utilized and modeled, and the analysis was conducted using the OpenLCA 2.0 software.

LCA is defined by the ISO 14040/14044 standard, which provides a framework for evaluating the environmental impacts of

Table 2 Chemical prices and global warming potentials for synthetic silk fiber production

Chemical	Price (USD per kg)	GWP (kg CO_2eq per kg)
Acetic acid	0.5	5.59
$C_{18}H_{36}N_4O_{11}$	0.05	0.1
$C_6H_5FeO_7$	0.16	0.02
$Cl_2COH_{12}O_6$	0.176	29.87
$CuCl_2$	0.05	0.04
EDTA	0.12	4.18
Glucose	0.5	1.29
Glycerol	1.06[a]	12
Grenadine hydrochloride	275	0.5
H_3BO_3	0.09	0.94
HFIP	130 (ref. 42)	10
Imidazole	7	5.73
IPTG	28 000[b]	0.5
Isopropanol	1.2	3.21
K_2HPO_4[c]	154	1.04
KH_2PO_4[d]	50	1.04
Methanol	0.6	0.54
$MgSO_4$	0.43[e]	0.41
$MnCl_24H_2O$	0.04	0.5
Na_2HPO_4	0.056	0.02
$Na_2MoO_4H_2O$	0.46	0.8
Na_2SO_4	0.0037	0.62
NaClO	0.5	0.02
Natural gas	0.000084	2.6[f]
NH_4Cl	0.0017	1.52
Resin	40 000[g]	1.61
Tris	0.5	0.06
Tryptone	0.25	0.5
Urea	0.31[h]	1.65
Water	0.00012	0.00066
Yeast	7.3 (ref. 43)	0.026[i]
Yeast extract	0.04	0.5
$Zn(CH_3CO_2)_2$	0.072	0.51

Prices from Alibaba.com and GWP from EcoInvent 3.7 unless noted otherwise. [a] https://www.selinawamucii.com/. [b] https://www.sigmaaldrich.com/US/en/product/sial/i6758. [c] https://www.bioland-sci.com/index.php?main_page=product_info&products_id=1466. [d] https://www.calpaclab.com/di-potassium-hydrogen-phosphate-anhydrous-k2hpo4-1-kg/cp-33750632-1kg. [e] https://www.imarcgroup.com/magnesium-sulfate-pricing-report. [f] Energy information administration. [g] https://www.creativebiomart.net/ni-nta-agarose-397628.htm?gad_source=1. [h] https://tradingeconomics.com. [i] https://cofalec.com/wp-content/uploads/2022/03/20120327155707_Yeast_Carbon_Footprint_COFALEC_28english-version29.pdf.

a product or system.[45] The goal for this project is to evaluate the GWP of synthetic silk fibers. The scope is Cradle-to-Gate from resource production and collection to the manufacture of the final product at the facility gate. The inventory data are based on the EcoInvent 3.7.1 database and literature data employing the Allocation at the Point of Substitution (APOS) system. The impact allocation method is the displacement, or system expansion, method. The interpretation includes estimating the GWP and conducting sensitivity analysis.

Fig. 2 shows the system boundary for synthetic silk fiber production. The process starts with the collection of key materials and resources. Glycerol is available as a by-product of biodiesel production. It is also available from soap production and oil and fat processing. Batch and fed media chemicals are generally available commercially or produced within the facility. In this study, the cells were grown within the facility using a custom inoculum. Other chemicals and solvents were purchased commercially. The facility obtained heat and electricity from utilities, and we assume a US grid power mixture. The final fiber is sold into the US market. There are no by-products sold from this process. All waste streams are collected for treatment at a commercial wastewater treatment facility.

2.7. Machine learning fiber market value analysis

Predicting the market value of novel synthetic fibers is challenging, as traditional methods relying on expert judgment can be subjective. While external market factors play a role, a fiber's inherent value is fundamentally driven by its performance characteristics, directly reflected in key mechanical properties like tensile strength, elongation, and Young's modulus. These properties dictate a fiber's suitability for various applications, making a high-performing fiber inherently more valuable (*e.g.*, for aerospace or composites). To overcome the limitations of traditional valuation, we developed a machine-learning model that predicts the market price of synthetic silk fibers using these mechanical properties as input features. This data-driven approach, trained on data from Ashby plots (a standard material selection tool visualizing property–price relationships), offers a more objective and accurate valuation method than relying on subjective analogies, enabling better initial price estimations for novel materials.

Ashby plots[46] provide a valuable resource for training machine-learning models by offering a broad range of data points for both natural and synthetic fibers. The price data along with the respective properties are typically represented as elliptical *ranges* rather than discrete values on the Ashby plots. Moreover, in our case, we had a 4D ellipse based on ranges of price, tensile strength, elongation and Young's modulus of silk fiber.

We extracted data points *inside* this 4D ellipse and trained machine learning models using a neural network, decision tree, and multivariate regression for price prediction. The data points were extracted using two kinds of distributions (each as separate scenarios): multinormal and beta distributions (Fig. 3).

To exercise the machine learning model, we employed literature data gathered by Koeppel and Holland.[47] Their review paper collected protein concentration and fiber material properties from various studies covering regenerated silk fibroin (RSF) wet and dry spun fibers, recombinant silk wet spun fibers, and natural silks as the control. Mechanical fiber properties, reported during 1960–2016, indicate continuous improvements, especially after 2007, due to improvements in solvent choice, post-processing technology, and thinning of the fiber thickness. During this time, the fiber strength rose from approximately 2.5 cN per dtex to more than 50 cN per dtex, extensibility from 20% to more than 50%, and toughness from less than 50 MJ m^{-3} to more than 150 MJ m^{-3}. We collected fiber yield data from the original studies. We predicted fiber market values using the machine learning algorithm and evaluated the production costs based on the fiber yields.

The machine learning model employed here can be viewed as a highly non-linear variant of a hedonic price regression, in

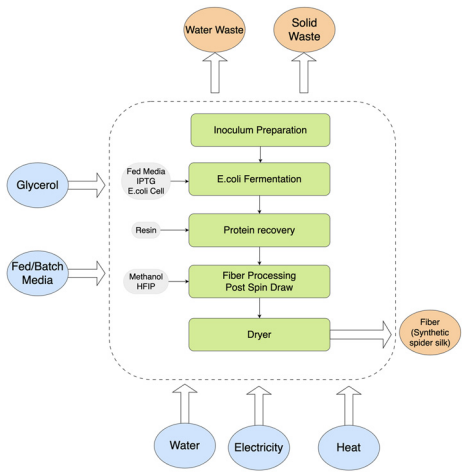

Fig. 2 Life cycle assessment system boundary for synthetic silk fiber production.

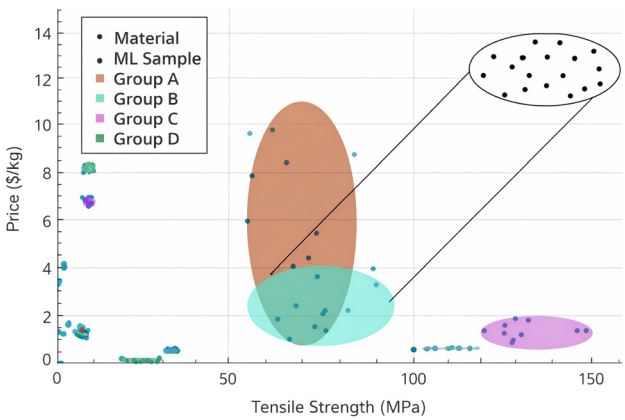

Fig. 3 A 2D representation of data point extraction for training machine learning models using Ashby plots.

which the goal is to estimate the relationship between product characteristics and observed prices. Under restrictive conditions, such models may permit recovery of consumers' marginal willingness-to-pay for individual characteristics.[48,49] However, in the absence of these conditions, the approach inherits several well-known econometric problems of hedonic pricing models, including sensitivity to the choice of characteristics, dependence on functional form assumptions, and, most importantly, the lack of parameter invariance.[50,51] This final limitation implies that coefficients estimated from reduced-form correlations are unlikely to remain stable under changes in the market structure or policy, undermining their usefulness for counterfactual analysis. In this case, the counterfactual is the introduction of fibers based on synthetic spider silk.

The choice of product characteristics—and the risk of omitting relevant ones—introduces the possibility of omitted variable bias through unobserved heterogeneity in the regression. In such cases, estimated coefficients may mistakenly attribute price variation caused by omitted characteristics to the observed ones. This problem not only undermines causal interpretation but also has negative implications for out-of-sample prediction performance.[52] Similarly, the choice of functional form imposes restrictions on how prices can depend on characteristics. The machine learning model helps address this concern by serving as a highly flexible non-linear approximator, capable of capturing complex relationships between characteristics and prices. Finally, the relationship between prices and characteristics in a hedonic model is a reduced-form statistical correlation rather than a structural model of supply and demand.[49,50,53,54] As a result, when the underlying market structure or policy environment shifts, the estimated parameters may no longer capture the true relationship between characteristics and prices. In other words, the model lacks policy invariance: coefficients that appear stable under one equilibrium regime can change when firms or consumers adjust their behavior in response to new conditions. For example, the introduction of a new and potentially disruptive product can alter substitution patterns, consumer valuations, and competitive dynamics in ways that differ from the original reduced-form estimates.

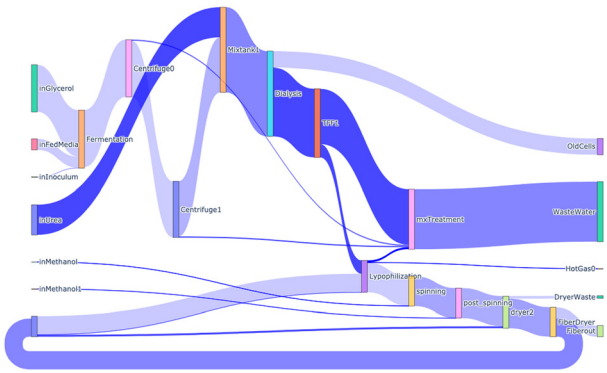

Fig. 4 Mass flows for 9000 tons per year of synthetic silk fiber production (27% of protein yield scenario).

3. Results and discussion

3.1. Material and energy balance

The Sankey diagram represents the mass and energy balance in the synthetic spider silk production design, showing how the input of glycerol has been transformed to synthetic spider silk and waste. Fig. 4 shows mass flows for the synthetic silk fiber production system. Material flow data are derived from BioSTEAM simulations under a 27% protein yield scenario, corresponding to the base case configuration. The process is designed to produce approximately 9000 metric tons of dry fiber annually. However, depending on the fermentation efficiency and protein recovery performance, production may range from 1200 tons to 9000 tons per year. The process employs 33 300 tons per year of glycerol (27% protein yield scenario), and 66 400 tons of urea are consumed annually, contributing to nitrogen supplementation during biomass and protein synthesis. These materials, both commodity-grade chemicals, are either commercially sourced or may be derived from waste streams such as used cooking oils (biodiesel side products) and food processing residues, supporting the potential for circular economy integration. The process also relies on smaller but essential volumes of inputs such as IPTG, antifoam agents, trace metals, and fed-batch media components. Notably, about 99 300 tons per year of extractive solution and process buffer are utilized, supporting various stages of cell lysis, purification, and dialysis. This intensive chemical demand underscores the importance of recovery and reuse strategies in reducing upstream environmental impacts.

The system generates approximately 72 182 tons of wastewater annually, which is routed to an on-site treatment facility. This volume reflects the aggregation of aqueous outflows from fermentation, centrifugation, purification, and drying stages. Proper treatment and reuse of this stream are essential for minimizing effluent burdens and meeting regulatory discharge thresholds.

Fig. 5 presents the energy flows for synthetic spider silk production. The total electricity demand of the process is approxi-

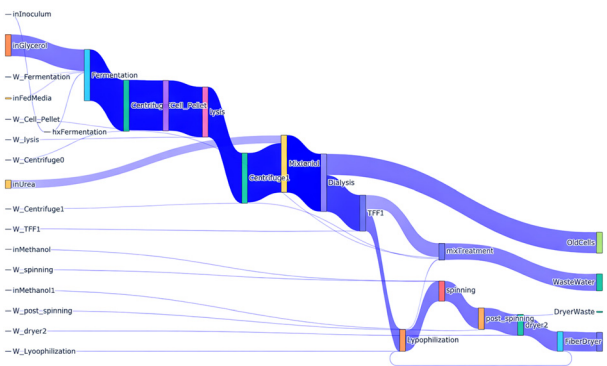

Fig. 5 Energy balance for 9000 tons per year of synthetic silk fiber production (27% of protein yield scenario).

mately 10.14 GWh per year, primarily driven by downstream processing and purification units. Among these, the fermentation unit is the most energy-intensive, consuming about 4.95 GWh per year. This is followed by the spinning and post-spinning operations, which collectively account for approximately 2.59 GWh per year, highlighting the energy burden of fiber formation and consolidation. The lyophilization step, essential for final product stabilization, consumes 0.87 GWh per year. Notably, centrifugal separations are also significant contributors, with Centrifuge0 and Centrifuge1 drawing a combined 1.06 GWh per year. Other contributors include the TFF unit (0.41 GWh per year) and Cell Pellet and lysis units, each consuming 32.2 MWh per year. The dryer system adds an additional 0.20 GWh per year.

3.2. Techno-economic analysis

3.2.1 Capital costs. The capital investment for the facility, producing 9000 tons of fiber per year, was estimated at $53 million. Fig. 6 shows the installed equipment cost breakdown. The fermentation unit is the most significant expenditure, amounting to $27 million. The spinning and post-spinning units represent the second-largest capital investment, totaling approximately $14.3 million, reflecting the complexity of solidifying and processing the spider silk fiber. The treatment tank, used for waste management, follows with an installed cost of about $4.5 million; wastewater treatment can be expensive for biobased industrial facilities due to the presence of contaminants requiring specialized treatment. Co-locating with a suitable wastewater treatment facility could significantly reduce capital costs. However, a detailed characterization of the waste streams would be required to evaluate this scenario. The centrifuge units (Centrifuge0 and Centrifuge1), along with associated steps like cell palletization and lysis, collectively cost around $1.2 million. Advanced purification and drying units, including tangential flow filtration (TFF), dialysis, and lyophilization, contribute to a combined installed cost of approximately $5.2 million. These units are essential for meeting stringent purity standards in the downstream processing of spider silk proteins.[41]

3.2.2 Annual operating costs. The annual operating cost analysis for this study presents a comprehensive breakdown of the expenses incurred in maintaining and running the facility. The total raw material cost stands at approximately $96 M per year, primarily driven by high-cost inputs such as resin ($32 M), glycerol ($32 M), urea ($18.6 M), and fed media ($14.6 M). Utilities contribute an additional $454 000 annually, which underscores the substantial energy requirements for operating the 30 bioreactors, centrifuges, and other equipment essential for the fermentation and purification processes. Labor costs are recorded at $144 000. This labor cost assumes that the facility operates like most fermentation facilities and does not depend on specialized labor. Some specialized tasks, like cell culture and waste characterization, can be expensed as needed. Maintenance and operation (OM) costs total $789 000 per year. Depreciation is included at $2.0 M, while income tax and return on investment (ROI) are recorded at $3.4 M and $10.9 M, respectively. Table 3 summarizes these annual operating expenditures, covering the consumables and ancillary materials necessary for daily operations. Property insurance and property tax costs are $549 000 and $109 000, respectively. Table 3 shows a summary of the annual operating costs.

3.2.3 Synthetic fiber minimum selling prices. The relationship between protein sequences, yield, productivity, and minimum selling price (MSP) is critical in determining the economic feasibility of synthetic spider silk production. As depicted in Fig. 5, the MSP varies significantly across different protein sequences, reflecting the impact of yield and productivity on production costs. The sequence 16xFGAILSS shows a higher yield of 27% and a productivity of 5.2 mg purified per gram of dry cell, resulting in a lower MSP. In contrast, the 128xFGAILSS sequence, with a lower yield of 4.5% and a productivity of 1.5 mg purified per gram of dry cell, has a higher MSP due to less efficient production, at a yield of 27% (16xFGAILSS), the MSP was $15 per kg of glycerol, as shown in Fig. 7. These findings highlight the importance of optimizing the protein yield and productivity to achieve cost-effective

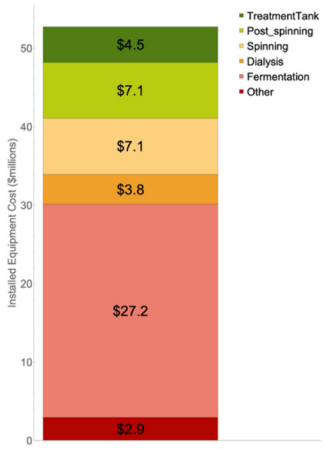

Fig. 6 Installed equipment costs 9000 tons per year of synthetic silk fiber production.

Table 3 Annual operating cost for synthetic silk fiber production

Cost factor	Annual operating cost ($)
In inoculum	1800
In glycerol	32 000 000
Other	524
In fed media	14 500 000
In grenadine hydrochloride	31 000
In resin	31 600 000
In urea	18 600 000
In HFIP	27 800
In methanol	19 800
Utilities	800 000
O&M	96 800
Depreciation	2 600 000
Income tax	3 820 000
ROI	11 700 000

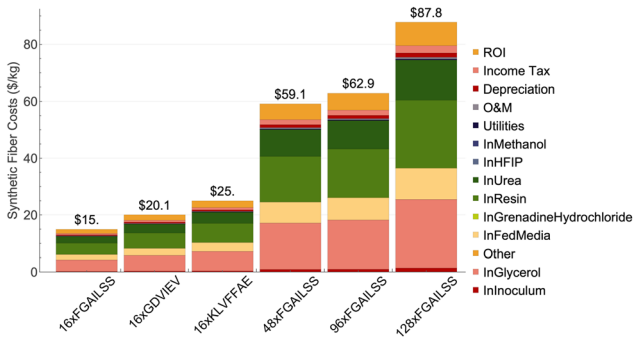

Fig. 7 Minimum selling price (MSP) of synthetic spider silk based on different protein sequences.

large-scale production. These estimates have an uncertainty of ±30%.

3.3. Life cycle assessment (LCA)

The GWP analysis for silk fiber production reveals a total emission of 17.39 kg CO_2-equivalent per kilogram of fiber for the 27% protein yield scenario, as depicted in Fig. 8. In comparison, the lowest-yield scenario analyzed, with a 4.5% protein yield, exhibited significantly higher emissions of 104 kg CO_2-equivalent per kilogram of fiber. This substantial difference underscores the pivotal role of optimizing protein yield in reducing environmental impacts. These findings align with previous studies, where substantial increases in protein expression levels led to dramatic reductions in emissions. For instance, a 10-fold increase in protein expression was shown to reduce emissions by 90%, from 572 kg CO_2-equivalent per kilogram to 55 kg CO_2-equivalent per kilogram,[10] emphasizing the importance of achieving higher yields to enhance the environmental efficiency. When compared to other fibers, silk fiber production at a 27% yield demonstrates notably lower emissions than natural silk, which emits approximately 58 kg CO_2-equivalent per kilogram. The higher emissions associated with natural silk are primarily due to the energy-intensive processes involved in mulberry cultivation and silk reeling. On the other hand, fibers such as jute and conventional cotton exhibit much lower emissions, with jute emitting between 1.05 and 1.50 kg CO_2-equivalent per kilogram and cotton around 1.70 kg CO_2-equivalent per kilogram. These lower emissions are attributed to the resource-efficient cultivation processes of these fibers, which rely heavily on natural rainfall and require minimal chemical inputs. Furthermore, jute contributes to carbon sequestration during its growth phase, and advancements in agricultural practices have enhanced the overall efficiency of cotton farming.[22]

The detailed contribution analysis, illustrated in Fig. 6, indicates that material consumption and electricity used during processing are the primary contributors to the overall GWP. Certain chemicals integral to the process, such as glycerol, urea, and fermentation-related inputs, significantly impact emissions. For instance, glycerol, a key component, dominates environmental impacts due to its high utilization rates and its associated adverse effects, including the formation of photochemical smog and contributions to greenhouse gas emissions. Optimizing the use of materials and improving the production efficiency can further reduce environmental impacts, reinforcing the sustainability of this production process and establishing it as a viable alternative in industry.[22,55]

The Tool for Reduction and Assessment of Chemicals and Other Environmental Impacts (TRACI) method was applied in the OpenLCA software to evaluate the environmental impact of synthetic spider silk production. Fig. 9 highlights nine environmental impact categories analyzed in this study, with the main contributing factors being the power consumption of five centrifuges, input materials (urea and glycerol), fermentation power consumption, and heat.

Among the contributors, the input materials, urea and glycerol, have a higher impact in the non-carcinogenics and Global Warming Potential (GWP) categories compared to other categories. In the non-carcinogenics category, these materials contribute over 80% of the total emissions, while in the GWP

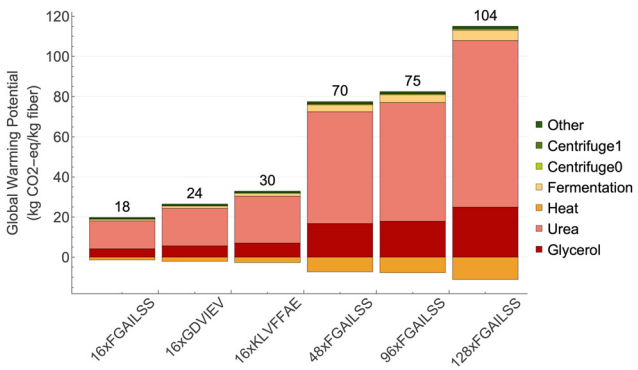

Fig. 8 Life cycle assessment (LCA) global warming potential (GWP) for synthetic spider silk production from six protein sequences. Silk fiber yields are reported in parentheses.

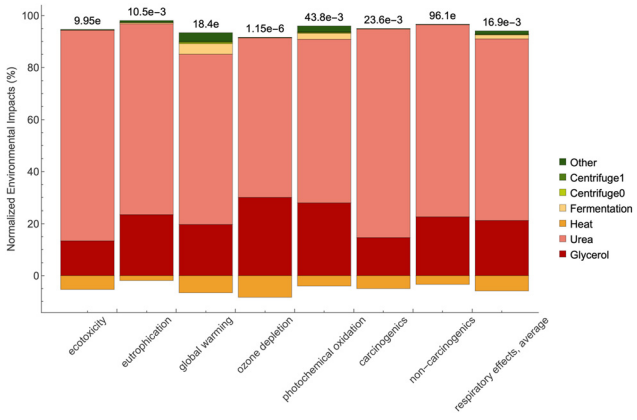

Fig. 9 Relative midpoint environmental impacts, including acidification, carcinogenics, ecotoxicity, eutrophication, global warming potential, non-carcinogenics, ozone depletion, photochemical oxidation, and respiratory effects of synthetic spider silk production (16xFGAILSS).

category, their contribution is over 60%. The energy use of the centrifuges is a minor contributor to most of the impact categories. Fermentation energy consumption has the smallest impact in the non-carcinogenics category compared to its role in other categories. LCA impact factor results are provided in Table S5.

3.4. Sensitivity analysis

To evaluate the economic feasibility of our synthetic spider silk production process, we conducted a comprehensive sensitivity analysis. This analysis focused on identifying the key techno-economic analysis (TEA) parameters that significantly impact the minimum product selling price (MPSP). The sensitivity analysis was performed by varying the key parameters within a range of ±20%. As illustrated in Fig. 10, the fiber yield, expressed in terms of kg fiber per kg glycerol, emerged as the most influential factor affecting the MPSP. A higher fiber yield substantially lowers the MPSP, emphasizing the importance of optimizing the fiber production process. The second most significant factor is the price of the feed media. Variations in feed media cost have a considerable impact on the overall production cost, highlighting the need for cost-effective media formulations or alternative nutrient sources to enhance economic viability. Additionally, raw material prices also play a critical role. Glycerol, in particular, is a major cost contributor. The analysis showed that the price of glycerol alone could significantly alter the MPSP, underscoring the necessity of either optimizing the glycerol usage or exploring cheaper alternatives. Conversely, the cost of natural gas exhibited a limited impact on the MPSP. This suggests that energy costs, while important, are less critical compared to raw material and feed media costs in this specific production process.

Fig. 11 shows the sensitivity of the LCA categories to changes to key parameters. Fiber yield, urea and glycerol emission factors are the most influential parameters. This result suggests that identifying alternative feedstock and green chemicals would significantly reduce the footprint of this process. Several technological factors that could improve this profile are the protein recovery, fiber spinning efficiency, and drying steps. They have varying material losses that are worth investigating in a future study.

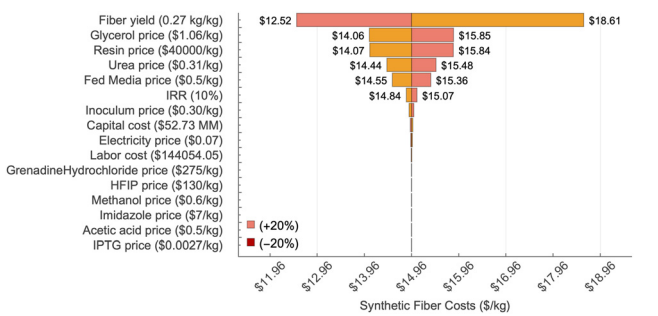

Fig. 10 Sensitivity analysis of synthetic spider silk production cost ($ per kg). Parameters are varied by ±20% from the baseline value shown in the plot.

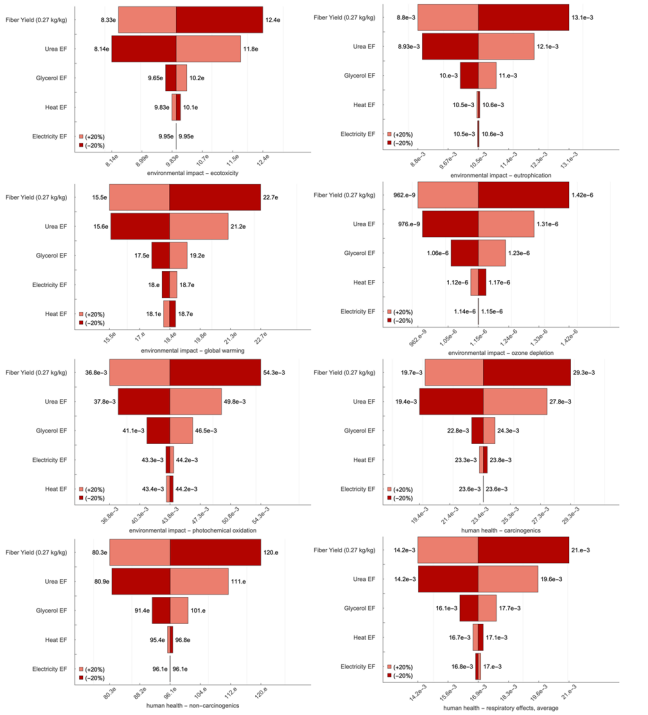

Fig. 11 Sensitivity analysis of LCA categories for synthetic spider silk production, showing fiber yield, urea, glycerol, electricity, and heat emission factors as the most influential parameters (±20% variation).

3.5. Machine learning fiber market value analysis

The neural network model with beta distribution demonstrated the best balance of predictive accuracy and the ability to handle the complexities of our dataset for this specific problem. While the datasets in Table 4 show good predictive performance, we recognize the inherent risks associated with neural networks, particularly their potential to overfit small or noisy datasets and obscure the direct relationship between input features and predicted prices. This trade-off between high predictive accuracy and model interpretability, along with considerations for generalizability, is critical. Despite these challenges, this approach was selected due to the neural network's demonstrated robustness to outliers and its capacity to capture the complex, non-linear relationships within the data more effectively than other models evaluated (Fig. 11). Further discussion on the specific robustness mechanisms employed and the quantitative trade-offs between accuracy and interpretability will be provided to strengthen the justification for this modeling approach. Fig. 11 shows a few examples of various combinations of distribution and machine learning models trained and their results.[56–63]

Fig. 12 compares the predicted price, derived from the Beta Distribution Neural Network, with the Minimum Selling Price (MSP) estimated by the TEA model. It is crucial to clarify that our predicted price represents a best-case benchmark for novel synthetic fibers, benchmarked against the historically observed market prices of *established* fibers with similar mechanical properties. While the model is trained on these historical

Table 4 Mean absolute percentage error (MAPE%) of fiber property prediction models across various models

	Normal distribution truncated – neural network	Beta distribution – neural network	Beta distribution – multi-variate regression
Matsumoto *et al.* (1996)[57]	19.19	15.2	16.26
Yao *et al.* (2002)[58]	19.93	12.92	17.4
Zhao *et al.* (2003)[59]	19.48	16.69	17.28
Um *et al.* (2004)[60]	18.74	18.01	19.48
Um *et al.* (2004)[60]	19.5	14.9	17.23
Marsano *et al.* (2005)[61]	19.62	16.34	19.41
Lee *et al.* (2007)[62]	19.84	15.23	17.58
Zhu *et al.* (2008)[56]	20.87	13.59	18.12
Sohn *et al.* (2009)[63]	18.69	13.24	15.7
Plaza *et al.* (2009)[64]	19.2	11.75	17.75
Plaza *et al.* (2009)[64]	16.66	22.86	20.99
Plaza *et al.* (2012)[67]	19.4	18.41	18.54
Plaza *et al.* (2012)[67]	20.18	19.39	20
Chen *et al.* (2017)[68]	15.84	11.77	27.55
Sun *et al.* (2012)[69]	20.57	24.72	19.76
Luo *et al.* (2014)[65]	21.03	25.22	22.2
Yue *et al.* (2014)[70]	19.92	22.82	20.49
Lazaris *et al.* (2002)[11]	18.92	20.39	22.06

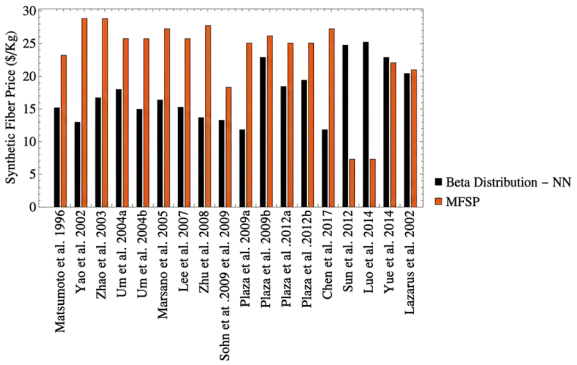

Fig. 12 Synthetic fiber price predictions based on various studies compared to the estimated minimum fiber selling prices.

market prices, reflecting a direct function of properties like tensile strength, elongation, and Young's modulus, it does not account for non-performance factors such as application context, certification, branding, market segmentation, or supply–demand dynamics, all of which influence the willingness-to-pay for truly novel materials. A predicted price exceeding the MSP suggests the potential technoeconomic profitability under the assumption of achieving market acceptance comparable to existing materials.

Three scenarios demonstrate this criterion for potential profitability: Plaza *et al.* (2009),[64] with a predicted price of \$25 per kg, *versus* an MSP of \$22.5 per kg; Yue *et al.* (2014)[70] at 24 kg^{-1} predicted *versus* \$23.5 per kg MSP; and Lazaris *et al.* (2002)[11] with a projected \$20 per kg predicted *versus* \$20.5 per kg MSP. Such close agreement between estimated prices and MSPs provides strong initial validation for the economic viability of synthetic fiber manufacture under these specific conditions. For all other scenarios, however, the predicted price is less than \$5 per kg, significantly lower than their respective MSPs, which are around \$20 per kg. This discrepancy suggests that, based on current yields and fiber properties, these scenarios are unlikely to be economically viable. Achieving profitability for these cases would necessitate either increased fiber yields or improved fiber properties (or a combination of both). The observed low predicted prices for these non-viable scenarios are consistent with the typical focus of laboratory-scale studies, which prioritize demonstrating technological feasibility and exploring novel materials over optimizing production yields.[11,56–58,60,62–66]

4. Conclusions

This research has established the economic and environmental potential for producing synthetic spider silk fibers through the host system *Escherichia coli* (*E. coli*). Through techno-economic assessment (TEA) and life cycle assessment (LCA), the most important drivers of the production process were determined. The TEA showed that synthetic spider silk fibers can be sold at a minimum sale price of \$14.97 per kg under optimal conditions, *e.g.*, high fiber yield and efficient use of raw materials. Raw materials and utilities, especially glycerol, were the major cost factors. Feed media cost optimization and fiber yield optimization were identified by sensitivity analysis as requirements to achieve maximum economic performance. The LCA outcome showed overall GHG emissions at 17.39 kg CO_2-equivalent per kilogram of fiber compared to 58 kg CO_2-equivalent per kilogram in the case of natural silk production. Major findings indicate the necessity for ongoing emphasis on genetic and process engineering to increase fiber yield, investigation of low-cost and renewable feedstocks, enhancing energy efficiency, and the use and recycling of co-products and wastes to realize additional environmental and economic gains.

Additionally, a machine learning-based fiber value analysis was performed in a bid to forecast the synthetic fiber price

based on different fiber material properties. Of the models attempted, a beta distribution-trained neural network provided the best balance of predictiveness and stability. The analysis revealed that the MFSP for some historical fiber reports was lower than the market value. This suggests that synthetic fibers could be competitive with market alternatives based on recent laboratory yields if they meet market specifications. Commercialization may require overcoming scale-up and technological challenges that are not fully addressed in this study. Future work should evaluate the potential for synthetic fibers to capture high-value markets like the medical and space industries. Machine learning and artificial intelligence could accelerate the discovery of genetic strains delivering high yield and quality fibers.

Author contributions

M. T.: formal analysis and writing – original draft; B. J.: methodology and writing – review & editing; L. P.: methodology and writing – review & editing; P. D.: formal analysis and writing – original draft; F. Z.: supervision, funding acquisition, and writing – review & editing; M. F.: supervision, funding acquisition, and writing – review & editing; M. M. W.: supervision, funding acquisition, and writing – review & editing.

Conflicts of interest

There are no conflicts to declare.

Data availability

Data for this article, including process models, lifecycle inventory, and results, are available at Zenodo (https://doi.org/10.5281/zenodo.17195350).

Supplementary Information (SI) is available providing lifecycle inventory data, stream properties and equipment information. See DOI: https://doi.org/10.1039/d5gc05082k.

Acknowledgements

We gratefully acknowledge the support of the National Science Foundation Growing Converge Program (Award Number 2219077). We thank the Sustainable Energy Systems Analysis (SESA) group at Iowa State University for their support and collaboration.

References

1 A. Rising, M. Widhe, J. Johansson and M. Hedhammar, *Cell. Mol. Life Sci.*, 2011, **68**, 169–184.
2 C. Radtke, C. Allmeling, K.-H. Waldmann, K. Reimers, K. Thies, H. C. Schenk, A. Hillmer, M. Guggenheim, G. Brandes and P. M. Vogt, *PLoS One*, 2011, **6**, e16990.
3 C. Allmeling, A. Jokuszies, K. Reimers, S. Kall, C. Y. Choi, G. Brandes, C. Kasper, T. Scheper, M. Guggenheim and P. M. Vogt, *Cell Proliferation*, 2008, **41**, 408–420.
4 A. Popescu, V. Şerban and H. N. Ciocan, New Trends in the Global Silk Production in the Period 2011–2022, Scientific Papers. Series "*Management, Economic Engineering in Agriculture and rural development*", 2024, vol. 24, pp. 775–786.
5 A. Seidel, O. Liivak, S. Calve, J. Adaska, G. Ji, Z. Yang, D. Grubb, D. B. Zax and L. W. Jelinski, *Macromolecules*, 2000, **33**, 775–780.
6 Y. Hsia, E. Gnesa, R. Pacheco, K. Kohler, F. Jeffery and C. Vierra, *J. Visualized Exp.*, 2012, 4191.
7 M. Stark, S. Grip, A. Rising, M. Hedhammar, W. Engström, G. Hjälm and J. Johansson, *Biomacromolecules*, 2007, **8**, 1695–1701.
8 J. Jeon, K. Z. Lee, X. Zhang, J. Jaeger, E. Kim, J. Li, L. Belaygorod, B. Arif, G. M. Genin, M. B. Foston, M. A. Zayed and F. Zhang, *ACS Appl. Mater. Interfaces*, 2023, **15**, 56786–56795.
9 J. L. Yarger, B. R. Cherry and A. Van Der Vaart, *Nat. Rev. Mater.*, 2018, **3**, 18008.
10 A. M. Edlund, J. Jones, R. Lewis and J. C. Quinn, *New Biotechnol.*, 2018, **42**, 12–18.
11 A. Lazaris, S. Arcidiacono, Y. Huang, J.-F. Zhou, F. Duguay, N. Chretien, E. A. Welsh, J. W. Soares and C. N. Karatzas, *Science*, 2002, **295**, 472–476.
12 C. H. Bowen, T. J. Reed, C. J. Sargent, B. Mpamo, J. M. Galazka and F. Zhang, *ACS Synth. Biol.*, 2019, **8**, 2651–2658.
13 C. H. Bowen, B. Dai, C. J. Sargent, W. Bai, P. Ladiwala, H. Feng, W. Huang, D. L. Kaplan, J. M. Galazka and F. Zhang, *Biomacromolecules*, 2018, **19**, 3853–3860.
14 J. Li, B. Jiang, X. Chang, H. Yu, Y. Han and F. Zhang, *Nat. Commun.*, 2023, **14**, 2127.
15 D. R. Whittall, K. V. Baker, R. Breitling and E. Takano, *Trends Biotechnol.*, 2021, **39**, 560–573.
16 G. Bhattacharyya, P. Oliveira, S. T. Krishnaji, D. Chen, M. Hinman, B. Bell, T. I. Harris, A. Ghazitabatabaei, R. V. Lewis and J. A. Jones, *Protein Expression Purif.*, 2021, **183**, 105839.
17 R. V. Lewis, M. Hinman, S. Kothakota and M. J. Fournier, *Protein Expression Purif.*, 1996, **7**, 400–406.
18 S. Salehi, K. Koeck and T. Scheibel, *Molecules*, 2020, **25**, 737.
19 M. Andersson, Q. Jia, A. Abella, X.-Y. Lee, M. Landreh, P. Purhonen, H. Hebert, M. Tenje, C. V. Robinson, Q. Meng, G. R. Plaza, J. Johansson and A. Rising, *Nat. Chem. Biol.*, 2017, **13**, 262–264.
20 A. Abbaspour, A. Jahed and A. Ahmadi, *Energy Sci. Eng.*, 2023, **11**, 2831–2850.
21 A. Jahed, A. Abbaspour and A. Ahmadi, *Sci. Prog.*, 2024, **107**, 00368504241265003.
22 V. Gonzalez, X. Lou and T. Chi, *Sustainability*, 2023, **15**, 7670.
23 B. Schmuck, G. Greco, T. B. Pessatti, S. Sonavane, V. Langwallner, T. Arndt and A. Rising, *Adv. Funct. Mater.*, 2024, **34**, 2305040.
24 R. Fan, K. Knuuttila, B. Schmuck, G. Greco, A. Rising, M. B. Linder and A. S. Aranko, *Adv. Funct. Mater.*, 2025, **35**, 2410415.

25 J. J. Graham, S. V. Subramani, X. Yang, T. M. Russell, F. Zhang and S. Keten, *Sci. Adv.*, 2025, **11**, eadr3833.
26 D. N. Breslauer, *Adv. Funct. Mater.*, 2025, **35**, 2408386.
27 G. Dutton, *Genet. Eng. Biotechnol. News*, 2024, **44**, 14–15.
28 S. Khan and R. Dandautiya, in *Environmental Engineering for Ecosystem Restoration*, ed. N. Vinod Chandra Menon, S. Kolathayar and K. S. Sreekeshava, Springer Nature Singapore, Singapore, 2024, vol. 464, pp. 243–252.
29 S. Liu, H. Liu, Y. Meng, Q. Li and L. Wang, *Fibres Text. East. Eur.*, 2022, **30**, 1–7.
30 A. M. Giacomin, J. B. Garcia, W. F. Zonatti, M. C. Silva-Santos, M. C. Laktim and J. Baruque-Ramos, *IOP Conf. Ser.: Mater. Sci. Eng.*, 2017, **254**, 192008.
31 A. Dutta, A.H. Sahir, E. Tan, D. Humbird, L.J. Snowden-Swan, P.A. Meyer, J. Ross, D. Sexton, R. Yap and J. Lukas, *Thermochemical research pathways with in situ and ex situ upgrading of fast pyrolysis vapors* (No. PNNL-23823), Pacific Northwest National Lab.(PNNL), Richland, WA (United States).
32 K. Kawajiri and K. Sakamoto, *Sustainable Mater. Technol.*, 2022, **31**, e00365.
33 K. Sanford, G. Chotani, N. Danielson and J. A. Zahn, *Curr. Opin. Biotechnol.*, 2016, **38**, 112–122.
34 S. V. Subramani, J. Li, K. Z. Lee, N. Fisher and F. Zhang, *Mater. Adv.*, 2024, **5**, 3506–3516.
35 C. H. Bowen, C. J. Sargent, A. Wang, Y. Zhu, X. Chang, J. Li, X. Mu, J. M. Galazka, Y.-S. Jun, S. Keten and F. Zhang, *Nat. Commun.*, 2021, **12**, 5182.
36 W. Bai, C. J. Sargent, J.-M. Choi, R. V. Pappu and F. Zhang, *Nat. Commun.*, 2019, **10**, 3317.
37 B. Dai, C. J. Sargent, X. Gui, C. Liu and F. Zhang, *Biomacromolecules*, 2019, **20**, 2015–2023.
38 E. Kim, J. Jeon, Y. Zhu, E. D. Hoppe, Y.-S. Jun, G. M. Genin and F. Zhang, *ACS Appl. Mater. Interfaces*, 2021, **13**, 48457–48468.
39 E. Merrow, K. Phillips and C. Myers, *Understanding cost growth and performance shortfalls in pioneer process plants*, RAND/R-2569-DOE, Rand Corp., Santa Monica, CA, 1981.
40 Y. Cortes-Pena, D. Kumar, V. Singh and J. S. Guest, *ACS Sustainable Chem. Eng.*, 2020, **8**, 3302–3310.
41 D. Humbird, R. Davis, L. Tao, C. Kinchin, D. Hsu, A. Aden, P. Schoen, J. Lukas, B. Olthof, M. Worley, D. Sexton and D. Dudgeon, *Process Design and Economics for Biochemical Conversion of Lignocellulosic Biomass to Ethanol: Dilute-Acid Pretreatment and Enzymatic Hydrolysis of Corn Stover*, 2011.
42 T. Bhattacharya, A. Ghosh and D. Maiti, *Chem. Sci.*, 2021, **12**, 3857–3870.
43 T. H. Kwan, Y. Hu and C. S. K. Lin, *J. Cleaner Prod.*, 2018, **181**, 72–87.
44 Y. K. Leong, P. L. Show, J. C.-W. Lan, H.-S. Loh, H. L. Lam and T. C. Ling, *Clean Technol. Environ. Policy*, 2017, **19**, 1941–1953.
45 International Organization for Standardization, 2006.
46 M. F. Ashby, in *Materials Selection and Design*, ed. G. E. Dieter, ASM International, 1997, pp. 266–280.
47 A. Koeppel and C. Holland, *ACS Biomater. Sci. Eng.*, 2017, **3**, 226–237.
48 S. Rosen, *J. Polit. Econ.*, 1974, **82**, 34–55.
49 D. Epple, *J. Polit. Econ.*, 1987, **95**, 59–80.
50 M. L. Cropper, L. B. Deck and K. E. McConnell, *Rev. Econ. Stat.*, 1988, **70**, 668.
51 N. V. Kuminoff, C. F. Parmeter and J. C. Pope, *J. Environ. Econ. Manag.*, 2010, **60**, 145–160.
52 J. K. Abbott and H. A. Klaiber, *Rev. Econ. Stat.*, 2011, **93**, 1331–1342.
53 T. Potrawa and A. Tetereva, *J. Bus. Res.*, 2022, **144**, 50–65.
54 N. V. Kuminoff, C. F. Parmeter and J. C. Pope, *J. Environ. Econ. Manag.*, 2010, **60**, 145–160.
55 M. F. Astudillo, G. Thalwitz and F. Vollrath, in *Handbook of Life Cycle Assessment (LCA) of Textiles and Clothing*, Elsevier, 2015, pp. 255–274.
56 Z. H. Zhu, K. Ohgo and T. Asakura, *eXPRESS Polym. Lett.*, 2008, **2**, 885–889.
57 K. Matsumoto, H. Uejima, T. Iwasaki, Y. Sano and H. Sumino, *J. Appl. Polym. Sci.*, 1996, **60**, 503–511.
58 J. Yao, H. Masuda, C. Zhao and T. Asakura, *Macromolecules*, 2002, **35**, 6–9.
59 C. Zhao, J. Yao, H. Masuda, R. Kishore and T. Asakura, *Biopolymers*, 2003, **69**, 253–259.
60 I. C. Um, H. Kweon, K. G. Lee, D. W. Ihm, J.-H. Lee and Y. H. Park, *Int. J. Biol. Macromol.*, 2004, **34**, 89–105.
61 E. Marsano, P. Corsini, C. Arosio, A. Boschi, M. Mormino and G. Freddi, *Int. J. Biol. Macromol.*, 2005, **37**, 179–188.
62 C. S. Ki, J. W. Kim, H. J. Oh, K. H. Lee and Y. H. Park, *Int. J. Biol. Macromol.*, 2007, **41**, 346–353.
63 S. Sohn and S. P. Gido, *Biomacromolecules*, 2009, **10**, 2086–2091.
64 G. R. Plaza, P. Corsini, E. Marsano, J. Pérez-Rigueiro, L. Biancotto, M. Elices, C. Riekel, F. Agulló-Rueda, E. Gallardo, J. M. Calleja and G. V. Guinea, *Macromolecules*, 2009, **42**, 8977–8982.
65 J. Luo, L. Zhang, Q. Peng, M. Sun, Y. Zhang, H. Shao and X. Hu, *Int. J. Biol. Macromol.*, 2014, **66**, 319–324.
66 X. Peng, Z. Liu, J. Gao, Y. Zhang, H. Wang, C. Li, X. Lv, Y. Gao, H. Deng, B. Zhao, T. Gao and H. Li, *Molecules*, 2024, **29**, 1025.
67 G. R. Plaza, J. Pérez-Rigueiro, C. Riekel, G. B. Perea, F. Agulló-Rueda, M. Burghammer, G. V. Guinea, and M. Elices, *Soft Matter*, 2012, **8**, 6015–6026.
68 J.-P. Chen, G.-C. Chen, X.-P. Wang, L. Qin and Y. Bai, *Nutrients*, 2017, **10**, 24.
69 F.-D. Sun, J.-H. Zhang, S.-F. Wang, W.-K. Gong, Y.-Z. Shi, A.-Y. Liu, J.-W. Li, J.-W. Gong, H.-H. Shang and Y.-L. Yuan, *Mol. Breed.*, 2012, **30**, 569–582.
70 Y. Yue, K. Liu, M. Li and X. Hu, *Carbon*, 2014, **77**, 973–979.